

Research Article

Model-Independent Bounds on Kinetic Mixing

Anson Hook, Eder Izaguirre, and Jay G. Wacker

Theory Group, SLAC National Accelerator Laboratory, Menlo Park, CA 94025, USA

Correspondence should be addressed to Jay G. Wacker, jgwacker@stanford.edu

Received 2 March 2011; Accepted 28 July 2011

Academic Editor: Ian Jack

Copyright © 2011 Anson Hook et al. This is an open access article distributed under the Creative Commons Attribution License, which permits unrestricted use, distribution, and reproduction in any medium, provided the original work is properly cited.

New Abelian vector bosons can kinetically mix with the hypercharge gauge boson of the Standard Model. This letter computes the model-independent limits on vector bosons with masses from 1 GeV to 1 TeV. The limits arise from the numerous e^+e^- experiments that have been performed in this energy range and bound the kinetic mixing by $\epsilon \lesssim 0.03$ for most of the mass range studied, regardless of any additional interactions that the new vector boson may have.

1. Introduction

The Standard Model (SM) successfully describes all known interactions of SM fermions and gauge bosons; however, there are several phenomena that motivate physics beyond the SM. Chief among these open questions is the identity of dark matter and its interactions with the SM. Recent anomalies in cosmic ray and direct detection experiments have motivated the exploration of new gauge interactions in a putative dark sector [1, 2]. New Abelian vector bosons provide one of the most robust portals for dark matter—SM interactions. The new vector boson can interact with the SM, even if no SM fermions are directly charged under the additional gauge symmetry. This interaction occurs via mixed kinetic terms between the SM's hypercharge field strength and the new Abelian field strength [3].

The Lagrangian for a kinetically mixed $U(1)$ theory is

$$\mathcal{L} = \mathcal{L}_{\text{SM}} - \frac{1}{4}F_{\mu\nu}^{\prime 2} - \frac{\sin e}{2}F'_{\mu\nu}B^{\mu\nu} + \frac{m_{A'}^2}{2}A_{\mu}^{\prime 2} + \tilde{g}J_{A'}^{\mu}A'_{\mu}, \quad (1.1)$$

where $F'_{\mu\nu}$ is the field strength for the new vector boson, $B^{\mu\nu}$ is the field strength for the SM hypercharge, and $J_{A'}^{\mu}$ encapsulates the interactions of the A' with fields in the dark sector. The mixed kinetic term is interesting for several reasons. First, it is a dimension 4 operator,

meaning that it can be generated at high energies without decoupling. Second, this coupling allows communication with a secluded sector that otherwise has no interactions with SM fields. These considerations have motivated a dedicated program to search for kinetically mixed vector bosons [4–7].

Most of the current program for discovering a kinetically mixed vector boson involves producing the state and searching for its subsequent decays. This method is promising, but has the drawback that it assumes that the searches can recognize the decay products of the A' . If the dark sector has states lighter than the A' , then the A' will preferentially decay to the dark sector over SM states because the kinetic mixing parameter almost always satisfies $\epsilon \ll \tilde{g}$. Searching for the A' by looking for the dark sector final states requires a wide-ranging search program because the dark sector may decay back to the SM in a variety of different ways, for example, lepton jets [8–12]. Model-independent searches are possible using completely inclusive searches, for example, $e^+e^- \rightarrow \gamma + X$, but these are challenging and few of these searches have actually been performed.

At low masses, the best model-independent bounds arise from the $(g - 2)$ measurements of the electron and muon [13]; however, the power of $(g-2)_\mu$ begins to weaken for $m_{A'} \gtrsim m_\mu$. At masses far above collider energies, the A' can be integrated out and its effects can be encapsulated in higher-dimension operators, most importantly S and T [14–16]. e^+e^- colliders have probed up to $\sqrt{s} = 207$ GeV and therefore, the effects of the A' cannot be parameterized as local higher-dimension operators for masses less than this energy scale.

This letter computes the model-independent constraints on the kinetic mixing parameter, ϵ , for masses between 1 GeV and 1 TeV by looking for the effects of virtual A' s on precision SM observables. This approach has the benefit of not requiring any knowledge of the decay modes of the A' and sets an upper limit on ϵ regardless of the behavior of the decay modes to the dark sector.

2. Kinetic Mixing

Kinetic mixing changes the mass eigenstates and interactions of the vector bosons. What follows is a brief synopsis of the results in [17], see also [18–21]. After diagonalizing the kinetic terms and going to the mass eigenstate basis, the SM neutral current interactions are modified. Absorbing the gauge coupling constants into the definition of the currents, the neutral current interactions are

$$\mathcal{L}_{\text{int}} = V_{\text{Gauge}}^\mu J_\mu = V_{\text{Mass}}^\mu \mathcal{M} J_\mu, \quad (2.1)$$

where the notation for the gauge and mass eigenstates is

$$V_{\text{Gauge}}^\mu = \begin{pmatrix} A^\mu \\ Z^{0\mu} \\ A'^\mu \end{pmatrix}, \quad V_{\text{Mass}}^\mu = \begin{pmatrix} A^\mu \\ Z^\mu \\ Z'^\mu \end{pmatrix}, \quad (2.2)$$

and the currents are

$$J^\mu = \begin{pmatrix} eJ_{EM}^\mu \\ \frac{g}{c_w} J_{Z^0}^\mu \\ \tilde{g} J_{A'}^\mu \end{pmatrix} \quad (2.3)$$

with the diagonalization matrix

$$\mathcal{M} = \begin{pmatrix} 1 & 0 & 0 \\ -c_w t_e s_\xi & s_w t_e s_\xi + c_\xi & \frac{s_\xi}{c_e} \\ -c_w t_e c_\xi & s_w t_e c_\xi - s_\xi & \frac{c_\xi}{c_e} \end{pmatrix}. \quad (2.4)$$

c, s, t stand for cosine, sine, and tangent, respectively, and c_w and s_w are the cosine and sine of the weak mixing angle. The photon's interactions are unaltered due to its residual gauge invariance. The angle ξ is defined as

$$\tan 2\xi = \frac{2\Delta(m_{Z'}^2 - m_{Z^0}^2)}{(m_{Z'}^2 - m_{Z^0}^2)^2 - \Delta^2}, \quad (2.5)$$

$$\Delta = -m_{Z^0}^2 \sin \theta_w \tan \epsilon$$

with $m_{Z^0} = m_{W^\pm} / \cos \theta_w$. After changing to the mass eigenstate basis, the physical mass of the Z^0, m_Z , is

$$m_Z^2 = \frac{m_{Z^0}^2 - m_{Z'}^2 \sin^2 \xi}{\cos^2 \xi} \quad (2.6)$$

and the physical mass of the new vector boson is

$$m_{Z'}^2 = m_{A'}^2 \frac{c_\xi^2}{c_e^2} + m_{Z^0}^2 s_\xi^2 \left(1 + \frac{s_w t_e}{t_\xi}\right)^2. \quad (2.7)$$

These corrections to the SM neutral currents and to the mass of the Z^0 place model-independent bounds on $(m_{Z'}, \epsilon)$. The next section describes the SM measurements that are sensitive to these modified neutral current interactions.

3. Precision SM Measurements

Virtual Z' exchange modifies measured observables such as Bhabha scattering, forward-backward asymmetry measurements, m_Z , and the total hadronic cross sections. The mass

of the Z^0 is the most powerful single measurement but the constraint is augmented by other measurements at and above the Z^0 pole. Additionally, if the Z' has a sizeable branching ratio back to the Standard Model, resonant production of the Z' bounds the parameter space at specific energies.

The strongest constraint on ϵ comes from the shift of the Z^0 mass [22]. Notice that ξ in (2.6) changes sign as $m_{Z'}$ goes through m_{Z^0} , meaning that the corrections to the Z^0 mass vanish at this point. Defining $\delta m = m_{Z'} - m_{Z^0}$, the correction to the Z^0 mass is given by

$$\frac{m_Z - m_{Z^0}}{m_{Z^0}} = -t_\xi^2 \frac{\delta m}{m_{Z^0}} + \mathcal{O}\left(\frac{\delta m^2}{m_{Z^0}^2}\right) \leq 2.5 \times 10^{-5}, \quad (3.1)$$

so that as $\delta m \rightarrow 0$, there is no bound on ϵ resulting from the measurement of m_Z . There is a reduction in the limits on ϵ for

$$m_{Z'} \simeq m_{Z^0} \pm 0.1 \text{ GeV}, \quad (3.2)$$

where other measurements must take over for the Z^0 mass measurement.

e^+e^- colliders measure the SM neutral current interactions and when $m_{Z'} \lesssim \sqrt{s} \leq m_{Z^0}$, the Z' couples dominantly to the electromagnetic current, which causes a kink to appear in the running of the fine structure constant. Differential Bhabha scattering measures $\alpha_{\text{EM}}(q^2)$ and there is a wealth of data from experiments such as OPAL [23], DELPHI [24], SLD [25], TASSO [26], CELLO [27], and TRISTAN [28]. As a result, the new vector boson changes the predictions for differential Bhabha scattering. All the experiments above have a large forward bin of $\cos\theta \gtrsim 0.9$, so only a small range of q^2 is probed at each experiment. The forward bin normalizes the luminosity and cannot be used as a constraint, thereby limiting the power of these measurements. Differential Bhabha scattering for $\sqrt{s} \leq m_{Z^0}$ is not useful but provides additional constraints at and above the Z^0 pole, where corrections to m_Z are less powerful.

In addition to differential Bhabha scattering, the forward-backward asymmetries for the bottom, charm, muon, and tau are measured at m_{Z^0} , effectively fixing $\alpha_{\text{EM}}(m_{Z^0})$ and $\sin^2\theta_w$ [29]. The modification to the SM neutral currents alters $\alpha_{\text{EM}}(m_{Z^0})$ and $\sin^2\theta_w$ and leads to a conflict with other SM predictions, most notably Γ_{Z^0} and $\sigma_{\text{had}} \equiv \sigma(e^+e^- \rightarrow \text{hadrons})$, that is, $\Gamma_{Z^0} = \Gamma_{Z^0}(\alpha_{\text{EM}}(m_{Z^0}), \sin^2\theta_w, G_F)$.

Resonant and on-shell production of the Z' can be relevant even if there is a small width directly back to the SM. The Z' has a decay width into the SM and dark sectors given by

$$\Gamma_{Z' \text{ SM}} \simeq \frac{\epsilon^2 g^2 m_{Z'}}{4\pi}, \quad \Gamma_{Z' \text{ dark}} \simeq \frac{\tilde{g}^2 m_{Z'}}{4\pi}. \quad (3.3)$$

The width of the Z' into the dark sector is unknown; however, given that bounds from the Z^0 mass set $\epsilon \lesssim \mathcal{O}(10^{-2})$ and \tilde{g} is bounded by $\mathcal{O}(1)$, there can be a detectable width for the Z' back into the SM. As a way to parameterize these effects, two different dark sector widths are used in setting limits

$$\Gamma_{Z' \text{ dark}} = \begin{cases} 10^{-2} m_{Z'} & \text{(wide),} \\ 0 & \text{(narrow).} \end{cases} \quad (3.4)$$

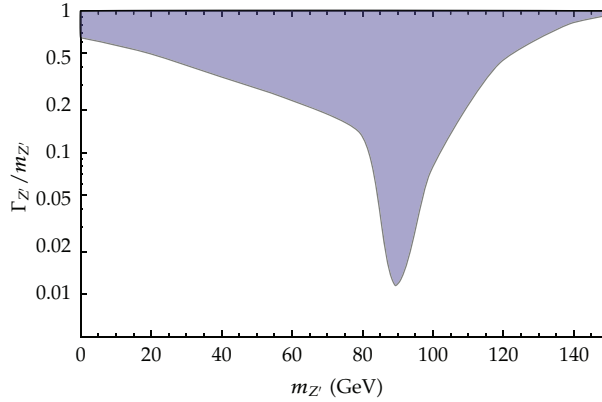


Figure 1: The model-independent upper bounds on $\Gamma_{Z'}$ arising from the line shape of the Z^0 .

On-shell production of the Z' is calculated using MadGraph 4.4.32 [30]. Only the interference between the Z' and the SM is explicitly computed by zeroing out the $|\text{SM}|^2$ and $|Z'|^2$ squared matrix elements. This results in a deviation from the SM that scales as e^2 and the calculations can be compared with measurements using the methods described in the next section.

The total hadronic cross sections, σ_{had} , are measured at LEP2 with $m_{Z^0} \leq \sqrt{s} \leq 207 \text{ GeV}$ [23, 24] as well as at many other experiments with $22 \text{ GeV} \leq \sqrt{s} \leq 64 \text{ GeV}$ [31]. These measurements provide additional bounds because the results from differential Bhabha scattering are not reported at every energy. While the error bars are large compared to the differential Bhabha scattering, resonant Z' production enhances sensitivity if $m_{Z'} \approx \sqrt{s}$. Radiative return processes involving the Z' could in principle constrain the theory for \sqrt{s} away from $m_{Z'}$; however, these never provide competitive measurements.

The Z^0 can have exotic decays into the hidden sector, and assuming that there are no mass thresholds in the hidden sector between m_{Z^0} and $m_{Z'}$, then

$$\Gamma_{Z^0 \text{ exotic}} \simeq t_\xi^2 \frac{m_{Z^0}}{m_{Z'}} \Gamma_{Z'}. \quad (3.5)$$

The Z^0 line shape measurement constrains Γ_{Z^0} in a model-independent manner giving a bound on $\Gamma_{Z'}$ [22]. The bound on the width of the Z' is shown in Figure 1.

In addition to precision e^+e^- measurements, direct searches at the Tevatron can produce on-shell Z' 's. This letter finds that the Tevatron's sensitivity is just beneath precision electroweak results even assuming $\Gamma_{Z' \text{ dark}} = 0$ [17, 32].

4. Results

The regions in the $(m_{Z'}, \epsilon)$ parameter space consistent with precision SM measurements are found by performing a global fit to the SM parameters. This letter uses a CL_s test that is a function of ϵ , $m_{Z'}$ and the Standard Model parameters, $\alpha_{\text{EM}}(m_{Z^0})$, G_F and $\sin^2\theta_w$. G_F is fit by

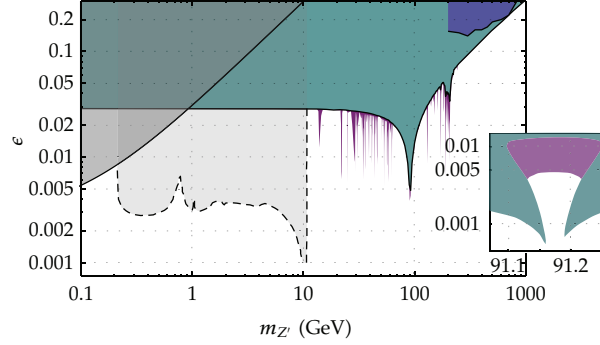


Figure 2: 95% CL exclusions in the $(m_{Z'}, \epsilon)$. The cyan region is excluded for a “wide” Z' and the purple region is for a “narrow” Z' . The blue region shows the bounds placed by CDF on direct production of Z' 's. The inset illustrates the constraints on $m_{Z'}$ near the Z^0 pole. The bound from the $(g-2)_\mu$ is shown in dark grey, and the light grey, dashed region shows the sensitivity from model-dependent BaBar searches.

μ decay and does not vary in practice. Most of the data is statistics dominated so that in the case where the signal predicts an excess of events, the CL_s simplifies into

$$CL_s(\epsilon, m_{Z'}; \text{SM Param}) = \prod_{\text{exp}} \frac{\sum_{n=0}^{n_{\text{obs}}} (e^{-N_{\text{sig}}} N_{\text{sig}}^n / n!)}{\sum_{n=0}^{n_{\text{obs}}} (e^{-N_{\text{back}}} N_{\text{back}}^n / n!)}. \quad (4.1)$$

Due to the high statistics, these Poisson summations can be approximated as gaussian integrals.

The advantage of using the CL_s method is that it is not diluted by superfluous measurements that have no *a priori* possibility of constraining a theory with a given $(m_{Z'}, \epsilon)$, only experiments that have a significant impact.

While superfluous measurements are ignored, measurements that only slightly affect the data can have a significant influence if there are enough of them. This can be illustrated by considering N experiments which all give the same result, only slightly different from the SM. A typical χ^2 analysis will never exclude the SM because the $\chi^2/\text{d.o.f.}$ is small. The CL_s method will eventually exclude the SM because $(1 - \epsilon)^N$ will be small for large N .

For $m_{Z'} \gg 200 \text{ GeV}$, the effects of the new vector boson can be encapsulated in terms of local operators and coincide with the precision electroweak analyses, for example, the S , T parameters [14–16] or more recently [33–35]. For $m_{Z'} \lesssim m_{Z^0}$, the bounds are close to those from [17–21], which only use the constraint from m_Z .

Figure 2 shows the 95% confidence level (CL) excluded regions in the $(m_{Z'}, \epsilon)$ plane obtained in this study. Wide Z' 's are best constrained by the mass of the Z^0 for most of the parameter space. The exception occurs near the Z^0 mass. The forward-backward asymmetries, Γ_{Z^0} , and σ_{had} augment the limits when the corrections to the Z^0 mass vanish and also for $m_{Z'} \approx 200 \text{ GeV}$ where LEP2 forward-backward measurements are more constraining than the Z^0 mass. Limits on narrow Z' 's are enhanced for $m_{Z'} \approx \sqrt{s}$ for the numerous e^+e^- experiments. The forward-backward asymmetries, hadronic cross section, and differential Bhabha scattering measurements provide the additional constraints. The peaks appearing in the exclusion region can be traced to experimental energies at which various experiments were conducted. The constraint on $m_{Z'}$ near the Z^0 is illustrated in the inset of Figure 2. For

comparison, the bounds from $(g - 2)_\mu$, and model-dependent $e^+e^- \rightarrow \gamma Z' \rightarrow \gamma \mu^+ \mu^-$ BaBar searches from [4, 36] are shown.

The main improvement of this work over previous papers is the use of lower energy experiments SLD, TASSO, CELLO, and TRISTAN to measure the running of α_{EM} and how it changes due to the addition of a new Z' boson. These low energy experiments augment the sensitivity to a new Z' boson, although the single strongest constraint is still the change in mass of the Z boson. These low energy experiments are sensitive to s channel production of the Z' and hence the width plays an important role. The width of the Z' depends on interactions with a hidden sector and cannot be a determined model, independently. Two different scenarios of the width of the Z' are considered. If the Z' is narrow, then there are many new small dips which are excluded (see Figure 2). If the Z' has a larger width, then the effects are washed out and the results are in agreement with [21].

The model-independent limits on kinetic mixing were computed in this letter and found to be $\epsilon \lesssim 0.03$ for most of the mass range studied, $1 \text{ GeV} < m_{Z'} < 200 \text{ GeV}$. The possible use of radiated return to place tighter constraints on Z' was investigated at both LEP1 and LEP2 energies; however, this channel did not help place tighter bounds on kinetic mixing. Even with the constraints found in this letter, there still is a vast parameter space available for a kinetically mixed vector boson to mediate interactions between a dark sector and the SM. The current program of searching for model-dependent decay modes at low energy experiments will augment these model-independent limits for $m_{Z'} \lesssim 10 \text{ GeV}$. For higher energies, only the LHC will provide additional information for $200 \text{ GeV} \lesssim m_{Z'} \lesssim 3 \text{ TeV}$ [17]. The relatively weak limits for $m_{Z'} \gtrsim 10 \text{ GeV}$ motivate new high intensity e^+e^- experiments to potentially discover new interactions of this form.

Acknowledgments

The authors would like to thank D. E. Kaplan, M. Lisanti, and M. Peskin for numerous useful conversations. A. Hook, E. Izaguirre, and J. G. Wacker are supported by the US DOE under contract number DE-AC02-76SF00515. A. Hook, E. Izaguirre, and J. G. Wacker receive partial support from the Stanford Institute for Theoretical Physics. J. G. Wacker is partially supported by the US DOE's Outstanding Junior Investigator Award.

References

- [1] N. Arkani-Hamed, D. P. Finkbeiner, T. R. Slatyer, and N. Weiner, "A theory of dark matter," *Physical Review D*, vol. 79, no. 1, 2009.
- [2] M. Pospelov and A. Ritz, "Astrophysical signatures of secluded dark matter," *Physics Letters B*, vol. 671, no. 3, pp. 391–397, 2009.
- [3] B. Holdom, "Two $U(1)$'s and e lunat charge shifts," *Physics Letters B*, vol. 166, no. 2, pp. 196–198, 1986.
- [4] R. Essig, P. Schuster, N. Toro, and B. Wojtsekhowski, "An electron fixed target experiment to search for a new vector boson A' decaying to e^+e^- ," *Journal of High Energy Physics*, no. 9, p. 1102, 2011, <http://www.springerlink.com/content/3u08526138805800/>.
- [5] J. D. Bjorken, R. Essig, P. Schuster, and N. Toro, "New fixed-target experiments to search for dark gauge forces," *Physical Review D*, vol. 80, no. 7, 2009.
- [6] R. Essig, P. Schuster, and N. Toro, "Probing dark forces and light hidden sectors at low-energy e^+e^- colliders," *Physical Review D*, vol. 80, no. 1, 2009.
- [7] M. Reece and L. -T. Wang, "Searching for the light dark gauge boson in GeV-scale experiments," *Journal of High Energy Physics*, vol. 2009, no. 7, 2009.
- [8] M. J. Strassler and K. M. Zurek, "Echoes of a hidden valley at hadron colliders," *Physics Letters B*, vol. 651, no. 5-6, pp. 374–379, 2007.

- [9] N. Arkani-Hamed and N. Weiner, "LHC signals for a superunified theory of dark matter," *Journal of High Energy Physics*, vol. 104, no. 12, 2008.
- [10] M. Baumgart, C. Cheung, J. T. Ruderman, L. T. Wang, and I. Yavin, "Non-abelian dark sectors and their collider signatures," *Journal of High Energy Physics*, vol. 2009, no. 4, 2009.
- [11] D. S.M. Alves, S. R. Behbahani, P. Schuster, and J. G. Wacker, "Composite inelastic dark matter," *Physics Letters B*, vol. 692, no. 5, pp. 323–326, 2010.
- [12] C. Cheung, J. T. Ruderman, L. -T. Wang, and I. Yavin, "Lepton jets in (supersymmetric) electroweak processes," *Journal of High Energy Physics*, vol. 2010, no. 4, 2010.
- [13] M. Pospelov, "Secluded U(1) below the weak scale," *Physical Review D*, vol. 80, no. 9, 2009.
- [14] M. E. Peskin and T. Takeuchi, "Estimation of oblique electroweak corrections," *Physical Review D*, vol. 46, no. 1, pp. 381–409, 1992.
- [15] B. Holdom, "Large corrections to electroweak parameters in technicolor theories," *Physics Letters B*, vol. 247, no. 1, pp. 88–92, 1990.
- [16] G. Altarelli and R. Barbieri, "Vacuum polarization effects of new physics on electroweak processes," *Physics Letters B*, vol. 253, no. 1-2, pp. 161–167, 1991.
- [17] S. Cassel, D. M. Ghilencea, and G. G. Ross, "Electroweak and dark matter constraints on a Z' in models with a hidden valley," *Nuclear Physics B*, vol. 827, no. 1-2, pp. 256–280.
- [18] B. Holdom, "Oblique electroweak corrections and an extra gauge boson," *Physics Letters B*, vol. 259, no. 3, pp. 329–334, 1991.
- [19] W. F. Chang, J. N. Ng, and J. M.S. Wu, "Very narrow shadow extra Z boson at colliders," *Physical Review D*, vol. 74, no. 9, 2006.
- [20] W. F. Chang and J. N. Ng, "Erratum: very narrow shadow extra Z boson at colliders," *Physical Review D*, vol. 79, no. 3, 1 pages, 2009.
- [21] D. Feldman, Z. Liu, and P. Nath, "Stueckelberg Z' extension with kinetic mixing and millicharged dark matter from the hidden sector," *Physical Review D*, vol. 75, no. 11, 2007.
- [22] C. Amsler, M. Doser, M. Antonelli et al., "Review of Particle Physics," *Physics Letters B*, vol. 667, pp. 1–6, 2008.
- [23] G. Abbiendi, C. Ainsley, and P. F. Åkesson, "Tests of the standard model and constraints on new physics from measurements of fermion-pair production at 189–209 GeV at LEP," *European Physical Journal C*, vol. 33, no. 2, pp. 173–212, 2004.
- [24] J. Abdallah, P. Abreu, W. Adam et al., "Measurement and interpretation of fermion-pair production at LEP energies above the Z resonance," *European Physical Journal C*, vol. 45, no. 3, pp. 589–632, 2006.
- [25] K. T. Pitts, *Electroweak coupling measurements from polarized bhabha scattering at the Z0 resonance*, Ph.D. thesis, 1994.
- [26] W. Braunschweig, R. Gerhards, F. J. Kirschfink et al., "A study of Bhabha scattering at PETRA energies," *Zeitschrift für Physik C*, vol. 37, no. 2, pp. 171–177, 1988.
- [27] H. J. Behrend, L. Criegee, J. H. Field et al., "Limits on electron compositeness from Bhabha scattering," *Zeitschrift für Physik C*, vol. 51, no. 2, pp. 143–148, 1991.
- [28] T. Arima, S. Odaka, K. Ogawa et al., "Precise measurement of Bhabha scattering at a center-of-mass energy of 57.77 GeV," *Physical Review D*, vol. 55, no. 1, pp. 19–39, 1997.
- [29] LEP Collaboration, "A combination of preliminary electroweak measurements and constraints on the standard model," <http://arxiv.org/abs/hep-ex/0312023>.
- [30] J. Alwall, P. Demin, S. De Visscher et al., "Mad graph/mad event v4: the new web generation," *Journal of High Energy Physics*, vol. 2007, no. 9, 2007.
- [31] P. Janot, "Closing the light sbottom mass window from a compilation of $e^+e^- \rightarrow \text{hadron}$ data," *Physics Letters B*, vol. 594, no. 1-2, pp. 23–34, 2004.
- [32] T. Aaltonen, A. Abulencia, J. Adelman et al., "Search for new physics in high-mass electron-positron events in $p\bar{p}$ collisions at $\sqrt{s}=1.96$ TeV," *Physical Review Letters*, vol. 99, no. 17, 2007.
- [33] R. Barbieri, A. Pomarol, R. Rattazzi, and A. Strumia, "Electroweak symmetry breaking after LEP1 and LEP2," *Nuclear Physics B*, vol. 703, no. 1-2, pp. 127–146, 2004.
- [34] Z. Han and W. Skiba, "Effective theory analysis of precision electroweak data," *Physical Review D*, vol. 71, no. 7, pp. 1–12, 2005.
- [35] ALEPH Collaborations, DELPHI Collaborations, L3 Collaborations, OPAL Collaborations, and SLD Collaborations, "Precision electroweak measurements on the Z resonance," *Physics Reports*, vol. 427, no. 5-6, pp. 257–454, 2006.
- [36] B. Aubert et al., "Search for a narrow resonance in e^+e^- to four lepton final States," in *Proceedings of the 24th International Symposium on Lepton-Photon Interactions at High Energy (LP '09)*, Hamburg, Germany, 2009.

The Hindawi logo consists of two interlocking loops, one blue and one green, forming a stylized infinity symbol.

Hindawi

Submit your manuscripts at
<http://www.hindawi.com>

